

Supplementary Material

ROS mediated cytoplasmic stiffening impairs the phagocytic ability of the macrophage

Mahesh Agarwal, Parijat Biswas, Anindita Bhattacharya and Deepak Kumar Sinha*

School of Biological Sciences, Indian Association for the Cultivation of Science, Jadavpur, Kolkata-32

*corresponding author: bcdks@iacs.res.in

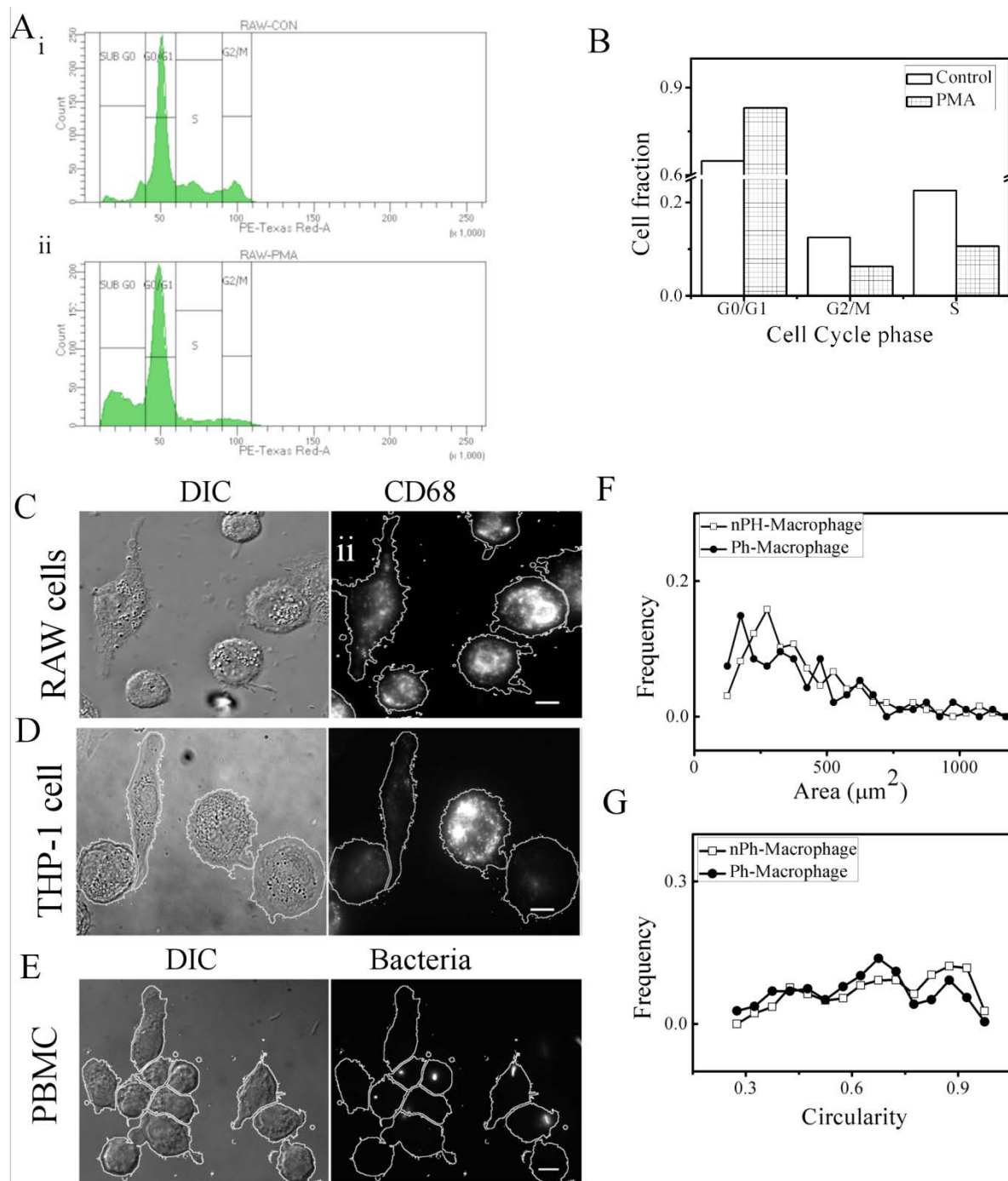


Figure S1: Phenotypic variability in macrophages. **A** Flow cytometric analysis of RAW 264.7 cells reveal that PMA treatment induces cell cycle arrest, as evident in A-i,ii. **B** Cell population fraction in each cell cycle phase is quantified from FACS data, which implies that post two days of PMA (50ng/mL) treatment, majority of the cells are arrested at G0/G1 phase. **C** and **D** show DIC and immunofluorescence images for CD68 marker in RAW264.7 (**C**) and THP-1 (**D**) respectively. **E** PBMC cells incubated with RFP expressing bacteria show phagocytic cells. **F** Plot depicts the distribution of spreading area of PH-Macrophages and nPH-Macrophages. **G** Plot depicts the variability in shape (circularity) of PH-Macrophages and nPH-Macrophages.

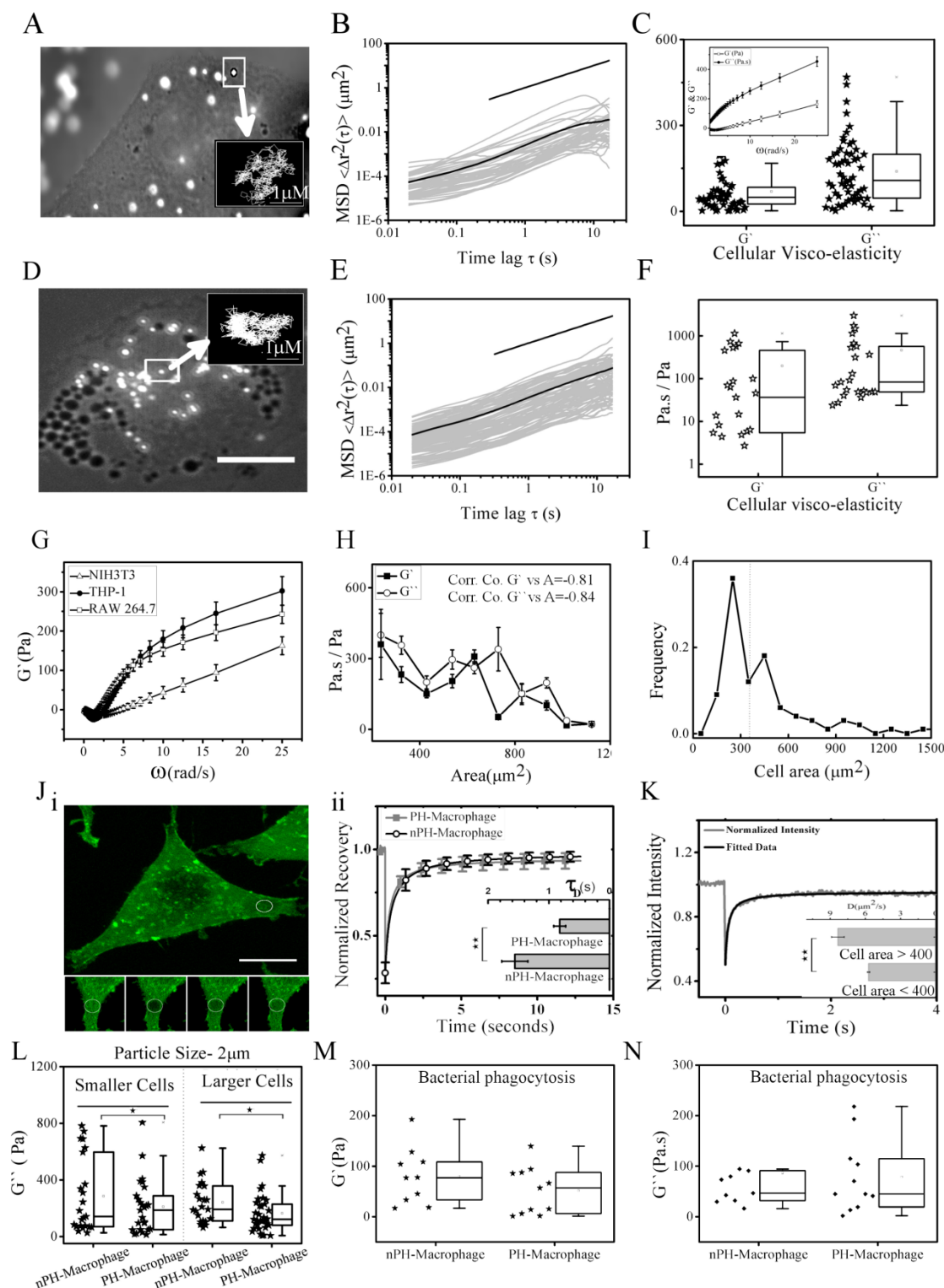
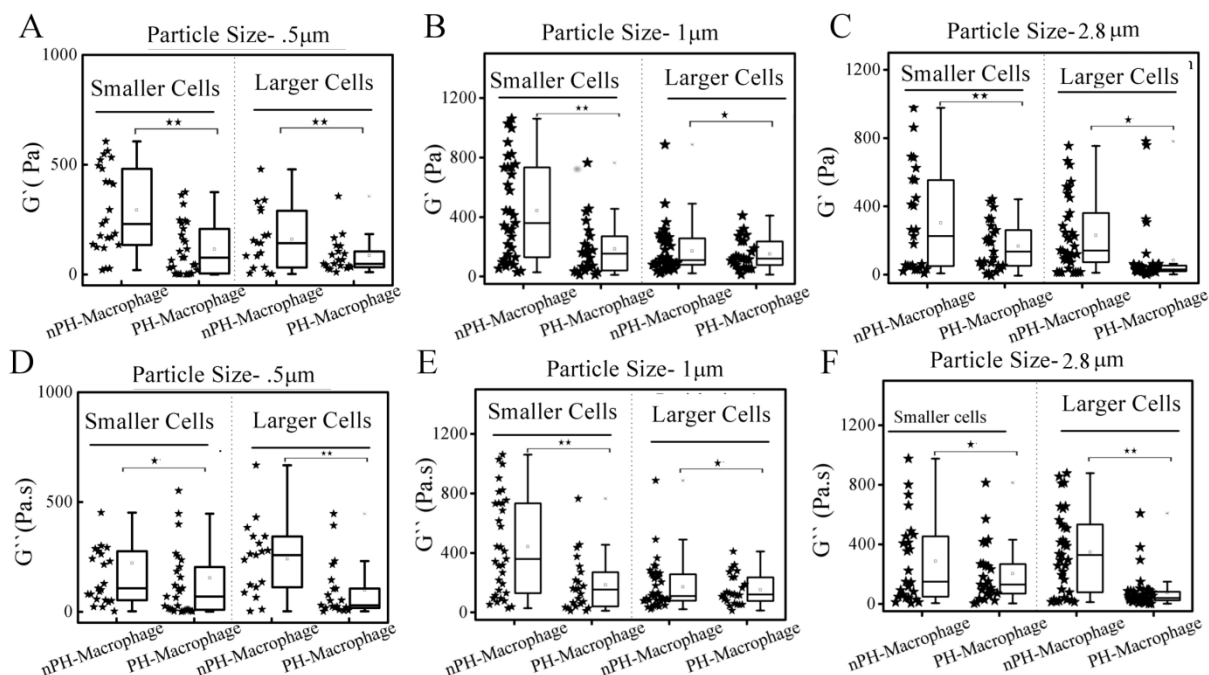


Figure S2: Macrophages show size dependent variation in cellular viscoelasticity. A Fluorescence images of 200nm carboxylated polystyrene beads mechanically injected into NIH3T3 fibroblasts for particle tracking microrheology experiments. The cell was simultaneously trans-illuminated with low intensity white light to depict the cell boundaries. Representative trajectory of a single bead (within white box) is shown at the right top of images (inset). **B** The Mean square displacement (MSD) (Gray lines) and ensemble average of MSD (bold black line) of beads embedded into the cytoplasm with respect to lag time (τ)

are shown. **C** A box plot depicting the elastic moduli (G') and viscous moduli (G'') of NIH3T3 cells measured with 200nm beads at a $\omega=10$ Hz. Inset depicts the average elastic modulus (G') and viscous modulus (G'') of NIH3T3 cells at different frequency (data from 52 cells). **D** Fluorescence images of 200nm carboxylated polystyrene beads mechanically injected into differentiated THP-1 cells (the cell was simultaneously trans-illuminated with low intensity white light to depict the cell boundaries). Representative trajectory of a single bead (within white box) is shown at the right top of images (inset). **E** The Mean square displacement (MSD) (Gray lines) and ensemble average of MSD (bold black line) of beads embedded into the cytoplasm with respect to lag time (τ) are shown. **F** A box plot depicting the elastic moduli (G') and viscous moduli (G'') of THP-1 cells measured with 200nm beads at a $\omega=10$ Hz, (data for 29 cells). **G** Plot depicts the elastic moduli (G') of various cell lines (triangle-NIH3T3 cells, circle-THP-1 cells, square-RAW cells) at different frequency (ω). **H** Plot depicts the cell-to-cell variability in elastic moduli (G') for different cell type. **I** Graph represents distribution of cellular area in PMA treated RAW264.7 cells. The vertical dotted line passes through the median of the distribution. **J-i** is a representative image of a RAW264.7 cell transfected with actin-mEGFP. The white circle is the ROI (region of interest) for a FRAP experiment. Lower panel depicts the bleaching and subsequent recovery of intensity in the ROI during the FRAP experiment. **J-ii** depicts normalized recovery curves and characteristic diffusion times (inset) of actin-mEGFP in PH-Macrophages and nPH-Macrophages when challenged with bacteria. Paired 't' tests were used to assess significance between recovery timescale (τ_D , in seconds) of aPR-Macrophages and the iPR-Macrophages ;* $P<0.05$, ** $P<0.01$, *** $P<0.001$. **K** FRAP experiments to investigate cytoplasmic viscosity in the small and large cells. The plot represents normalised recovery curves in RAW264.7 macrophages expressing mEGFP. Inset in lower right corner depicts the quantification of mEGFP diffusion rate (D , in $\mu\text{m}^2/\text{s}$) in RAW264.7 macrophage with area smaller and larger than $400\mu\text{m}^2$. Paired 't' tests were used to assess significance between recovery timescale (τ_D , in seconds) of smaller Macrophages and larger Macrophages ;* $P<0.05$, ** $P<0.01$, *** $P<0.001$. **L** shows viscous moduli (G'') of PH-Macrophages and nPH-Macrophages in the small ($<400\mu\text{m}^2$) and large ($>400\mu\text{m}^2$) regime upon incubation with beads of size $2\mu\text{m}$. **M**, **N** plots compare the elastic (**M**) and viscous (**N**) moduli of PH-Macrophage and nPH-macrophage when the cells were challenged with bacteria. Paired 't' tests were used to assess significance between the rheology of PH-Macrophage and nPH-Macrophage * $P<0.05$, ** $P<0.01$, *** $P<0.001$. The box represents the 25–75th percentiles, and the median is indicated. The whiskers show the complete range from minimum to aximum values. Points on the left side of graph show all values.

RAW 264.7 Macrophages day2 post PMA treatment



THP-1 Macrophages day3 post PMA treatment

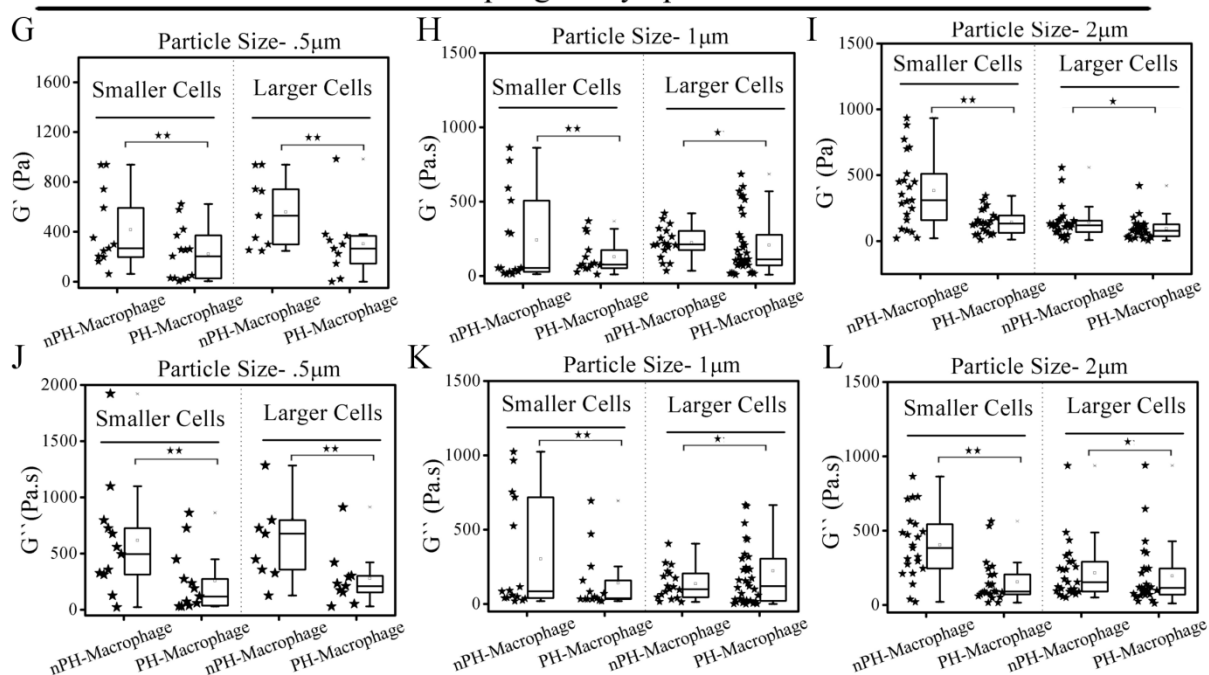


Figure S3: Cytoplasmic viscoelasticity of macrophages determine its phagocytic ability
A-C Cytoplasmic G' of smaller (<400 μm) and larger (>400 μm), PH-Macrophage and nPH-Macrophages challenged with beads (particle) of different sizes 0.5 μm (A), 1.0 μm (B) and 2.8 μm (C) in RAW264.7 cells. **D-F** Cytoplasmic G'' of smaller (<400 μm) and larger (>400 μm), PH-Macrophage and nPH-Macrophages challenged with beads (particle) of different sizes (0.5 μm (D), 1.0 μm (E) and 2.8 μm (F) in RAW264.7 cells. **G-I** Cytoplasmic G' of smaller (<400 μm) and larger (>400 μm), PH-Macrophage and nPH-Macrophages

challenged with beads (particles) of different sizes ($0.5\mu\text{m}$ (G), $1.0\mu\text{m}$ (H) and $2\mu\text{m}$ (I in THP-1 cells. **J-L** Cytoplasmic G'' of smaller ($<400\mu\text{m}$) and larger ($>400\mu\text{m}$), PH-Macrophage and nPH-Macrophages challenged with beads (particle) of different sizes ($0.5\mu\text{m}$ (D), $1.0\mu\text{m}$ (E) and $2\mu\text{m}$ (F) in THP-1 cells. Paired 't' tests were used to assess significance between the rheology of PH-Macrophage and nPH-Macrophage $*P<0.05$, $**P<0.01$, $***P<0.001$. The box represents the 25–75th percentiles, and the median is indicated. The whiskers show the complete range from minimum to maximum values. Points on the left side of graph show all values.

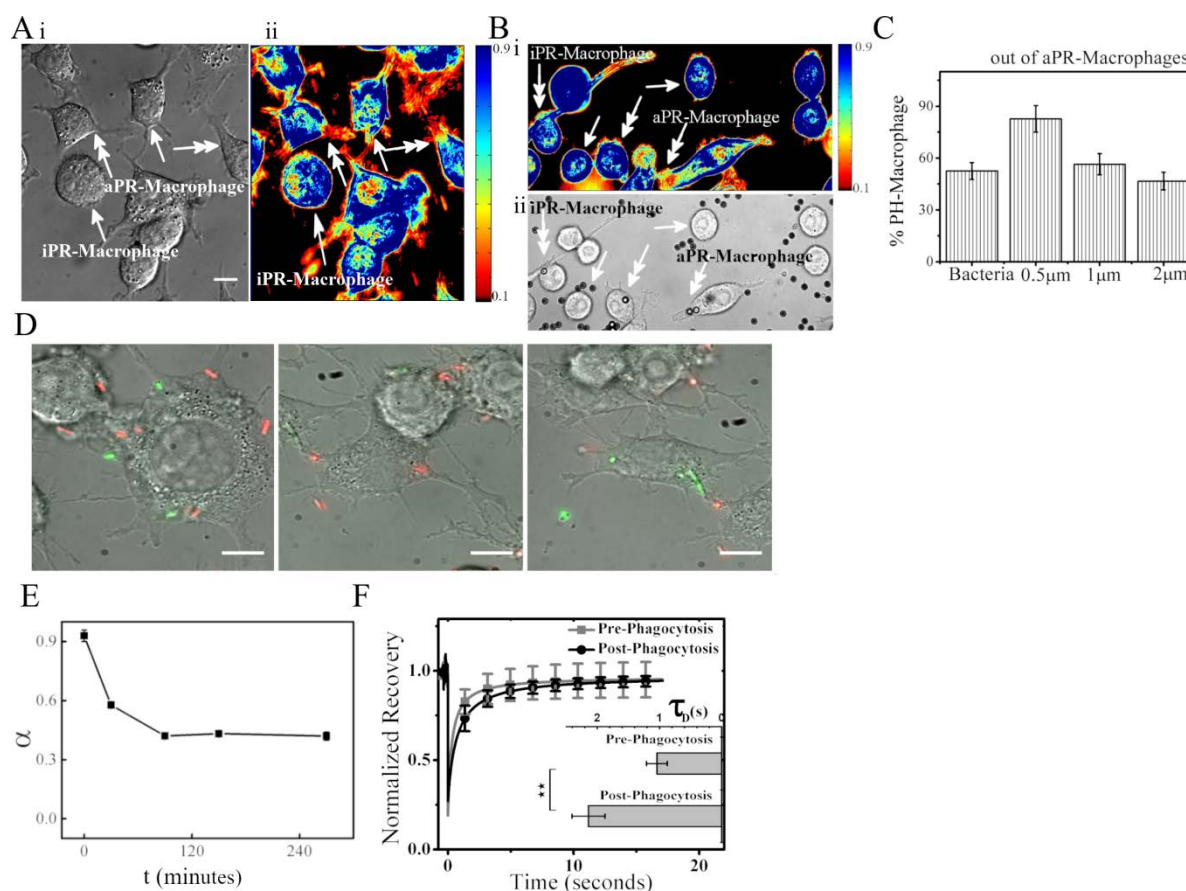


Figure S4: **A** depicts DIC (**i**) and sd images (**ii**) of DIC time lapse for Raw264.7 macrophage cells. The colour scheme in sd images is a measure of cell movement (see colour bar). The single headed arrow indicates iPR-Macrophage and double headed arrow indicates aPR-macrophage cells. **B** depicts sd images of DIC time lapse (**i**) for Raw264.7 macrophages. The single headed arrows indicate iPR-Macrophage and double headed arrows indicate aPR-macrophages. **B-ii** shows the DIC images of RAW264.7 macrophages incubated with $2.8\mu\text{m}$ sized particles that have undergone phagocytosis assay (The single headed arrows indicate nPH-Macrophage/iPR-Macrophage and double headed arrows indicate PH-macrophage/aPR-Macrophage cells). **C** Plot shows that propensity of phagocytosis is dependent on the size and nature of the objects being engulfed. **D** Images show the three outcomes of challenging RAW

264.7 cells with both RFP and GFP expressing bacteria. The RFP bacteria were added initially and then the GFP bacteria were added at subsequent time points. Cells either engulf both Red and Green bacteria (**D**-left), or just engulf the Red bacteria (**D**-centre) or the Green bacteria (**D**-right). **E** shows that PH-Macrophages gradually lose their phagocytic ability after initial bead engulfment, evaluated by FACS. **F** shows FRAP recovery plots for phagocytic cells pre- and post- engulfment of bacteria, revealing that actin dynamics is attenuated in cells that have undergone phagocytosis. Paired 't' tests were used to assess significance between recovery timescale (τ_D , in seconds) of aPR-Macrophages and the iPR-Macrophages; * $P < 0.05$, ** $P < 0.01$, *** $P < 0.001$.

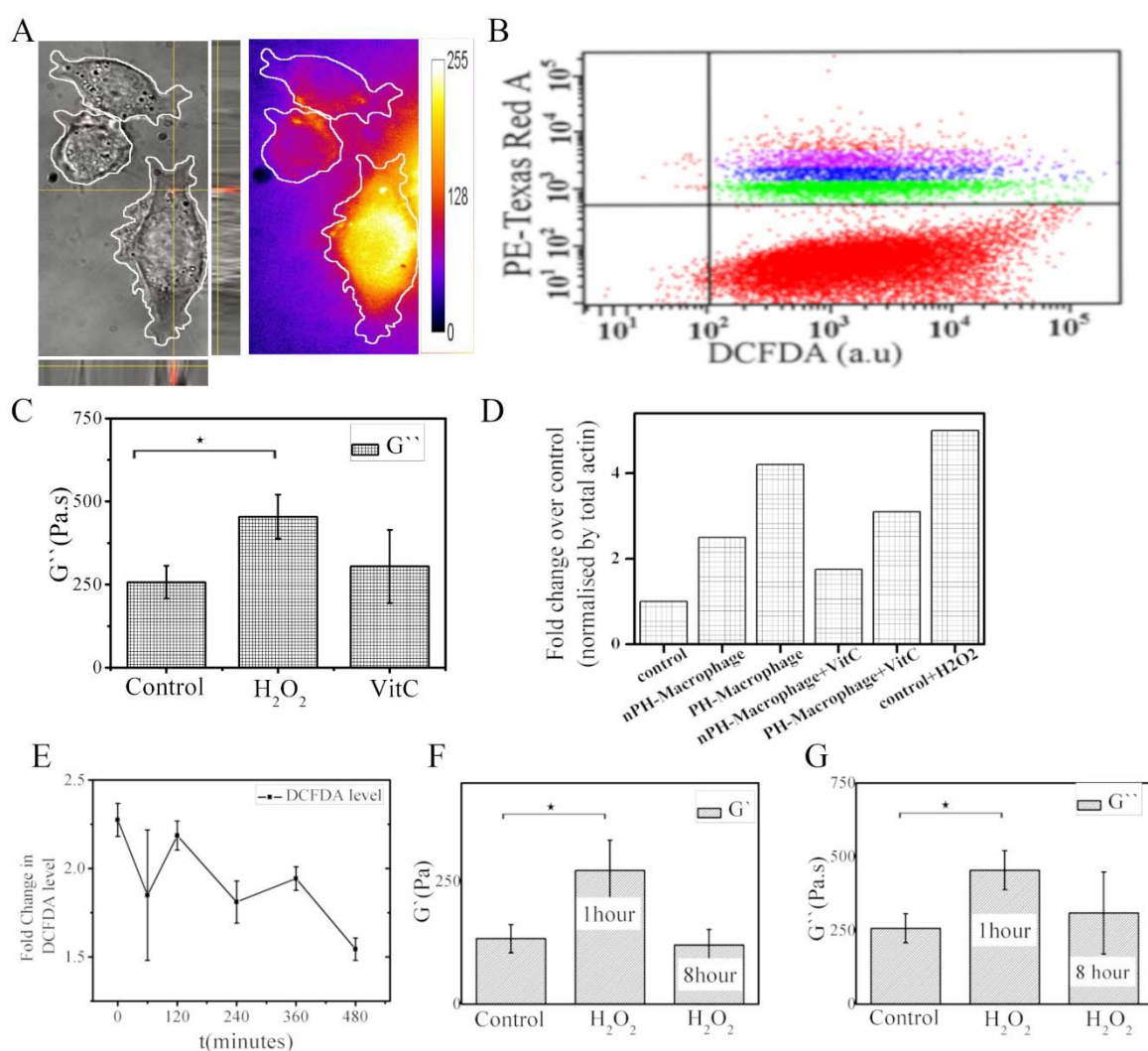


Figure S5: **A** DIC (left) and fluorescence (right) image of H₂DCFDA (10 μ M) treated RAW264.7 derived macrophage after phagocytosis assay with RFP bacteria. The colour bar (Fire LUT, ImageJ) depicts the H₂DCFDA fluorescence levels, and indicates higher ROS levels in phagocytic cells. **B** FACS analysis of phagocytic cells reveals that cells that have engulfed more beads have higher ROS levels. The subpopulations indicated by green, blue, purple and red have engulfed one, two, three and more than three beads, respectively in order.

C Cytoplasmic G'' of cells treated with 250 μ M H₂O₂ or 500 μ M Vitamin C for 1 hour. **D** Quantification of the IP-Western Blot of Figure 5-H in main text. **E** Fold change (with respect to unexposed cells) of intracellular ROS levels after phagocytosis assay. Time 0 min indicates 1 hour post incubation with bacteria. **F**, **G** show the cytoplasmic G' and G'' of macrophages post 1 hour and 8 hour of 250 μ M H₂O₂ treatment, respectively.

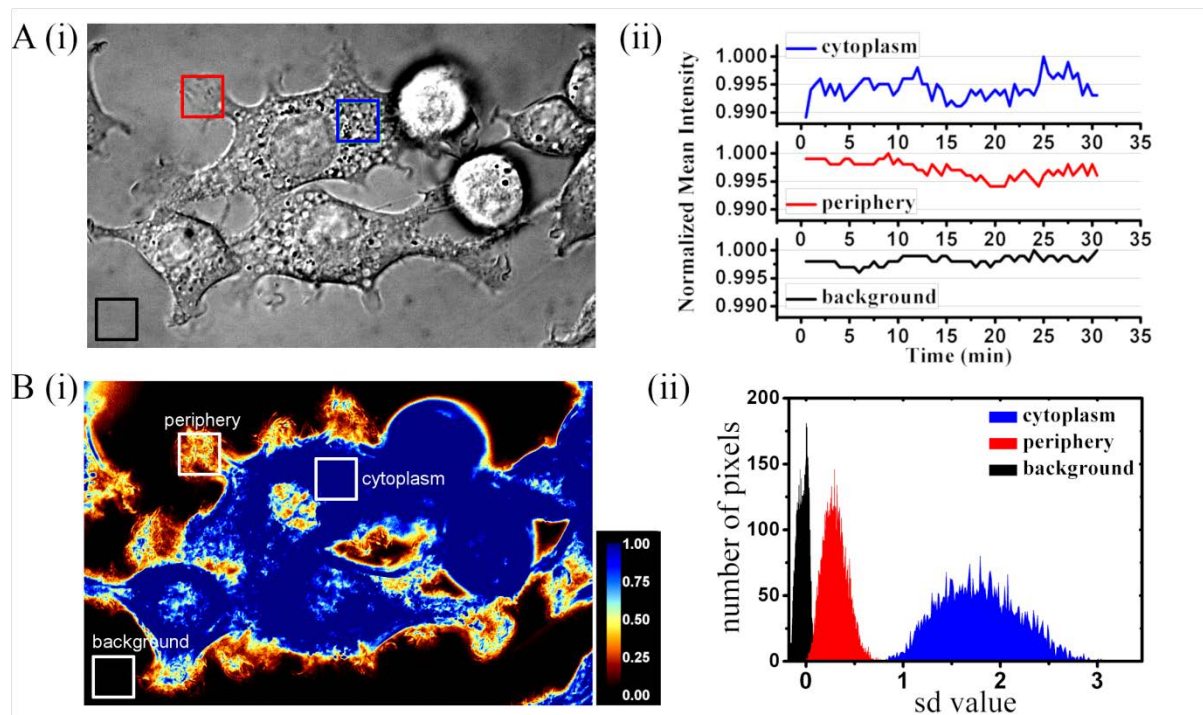
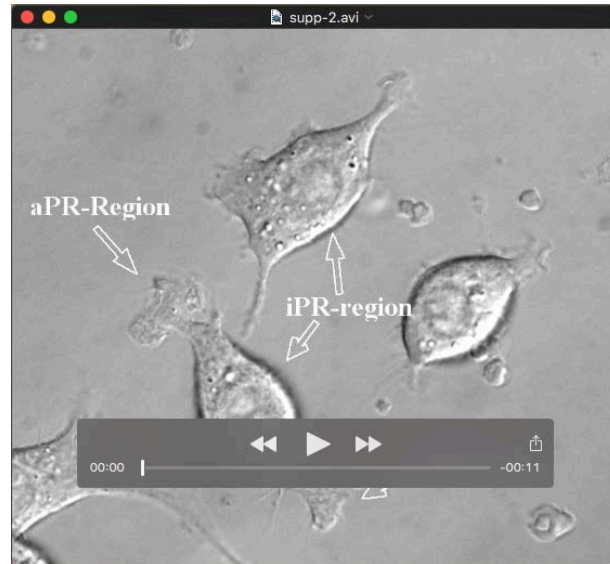
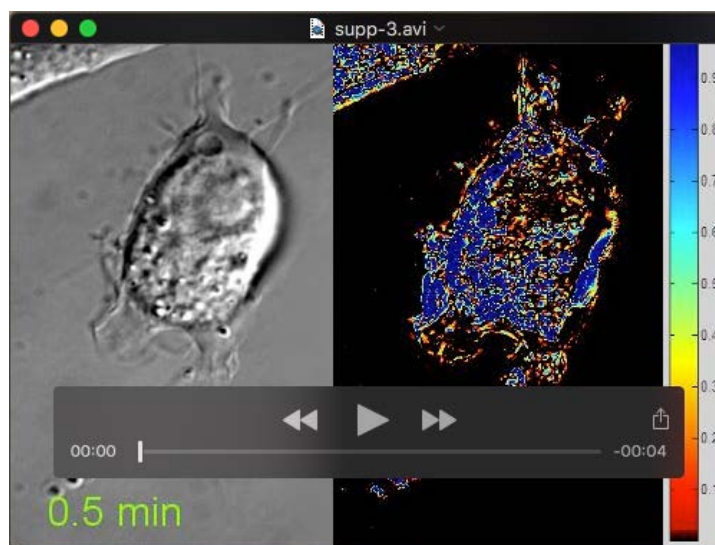


Figure S6: Standard Deviation (sd) Image Generation. **A (i)** A standard DIC image and its classification of background (black square ROI), cytoplasm (blue square ROI), and periphery (red square ROI) regime. **(ii)** The temporal fluctuations of mean intensity in the ROIs are plotted. **B (i)** shows the final sd image and **(ii)** shows the histogram of sd values in the ROIs at the three regimes, which are comprised of distinctly different sd values.

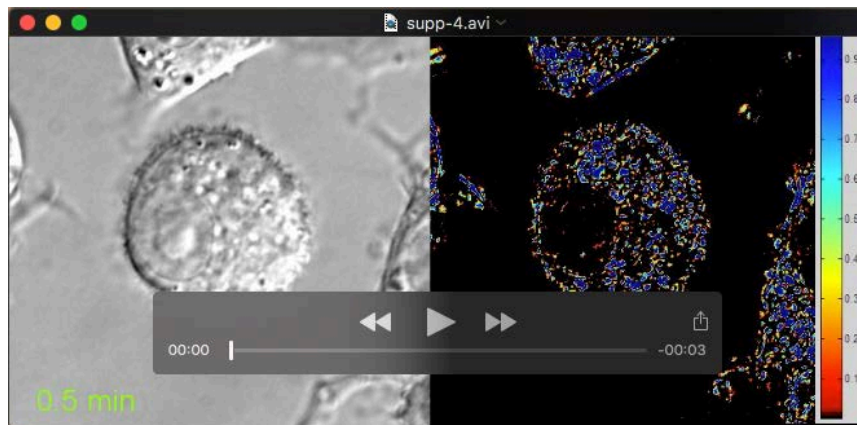
Movies



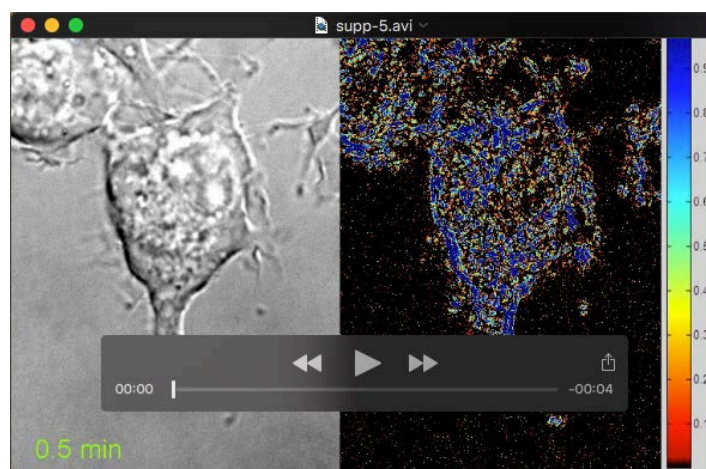
Movie 1: DIC time lapse images taken at 2frames/min of RAW264.7 cells performing phagocytosis. The aPR and iPR region have been indicated in the movie. The beads are being engulfed through the aPR-region.



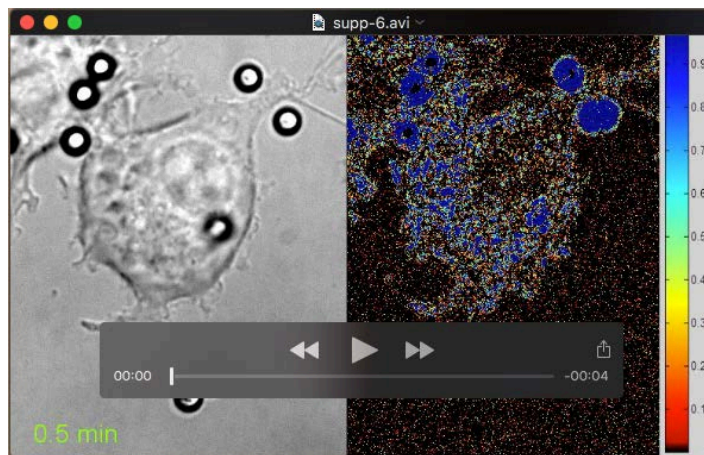
Movie 2: DIC time lapse images taken at 2frames/min and corresponding sd images depicting active protrusion retraction in aPR macrophage.



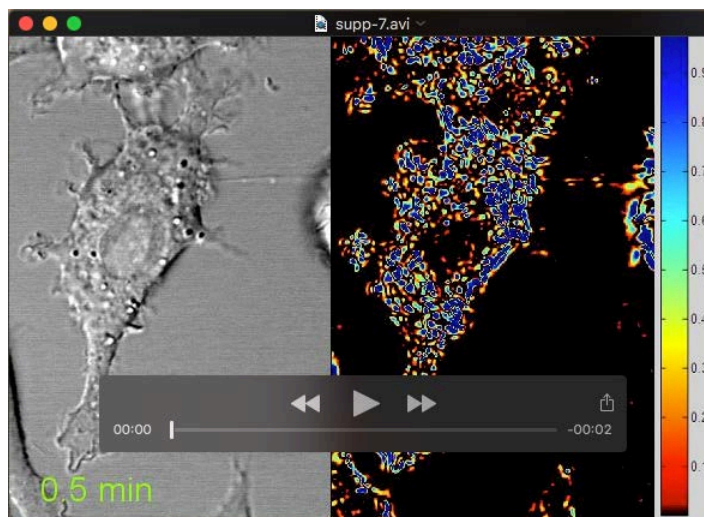
Movie 3: DIC time lapse images taken at 2frames/min and corresponding sd images depicting inactive protrusion retraction in iPR macrophage.



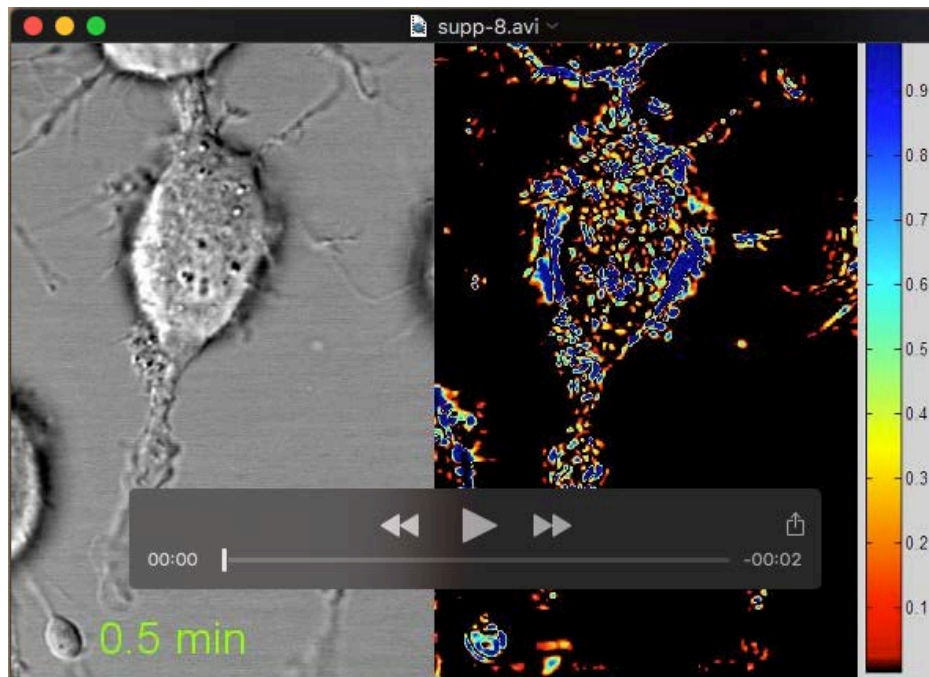
Movie 4: DIC time lapse images taken at 2frames/min and corresponding sd images of an aPR macrophage before bead engulfment.



Movie 5: DIC time lapse images taken at 2frames/min and corresponding sd images of the same cells in Movie 4 after bead engulfment. The protrusion-retraction activity is visibly lower.



Movie 6: DIC time lapse images taken at 2frames/min and corresponding sd images of a RAW264.7 macrophage before treatment with H_2O_2 (250 μm).



Movie 7: DIC time lapse images taken at 2frames/min and corresponding sd images of the same cells in Movie 6 after treatment with H_2O_2 (250 μm).